

Comparison of Performances of PMLSM Fed by Two Power Supplies

Jikai Si

School of Electrical Engineering & Automation, Henan Polytechnic University, Jiaozuo, China

Email: sijikai527@126.com

Xiaozhuo Xu, Haichao Feng, Baoyu Xu, Xudong Wang

School of Electrical Engineering & Automation, Henan Polytechnic University, Jiaozuo, China

Email: xxz@hpu.edu.cn, fhc@hpu.edu.cn, xuby@hpu.edu.cn, wangxd@hpu.edu.cn

Abstract—Inverters provided non-sinusoidal voltage or current, and the tooth-slot and winding distribution of the motor could lead to a mass of space harmonic components, severely deteriorating the motor performance. In order to know the cause of electromagnetic thrust and mover velocity fluctuation of low-velocity PMLSM fed by SPWM-VS, the steady-state performances of low-velocity PMLSM are analyzed in this paper. The performances of permanent magnet linear synchronous motor by sinusoidal pulse width module voltage source inverter (SPWM-VI-PMLSM) and sinusoidal voltage source inverter (S-VS) were researched used the field-circuit coupled adaptive time-stepping finite element method. The characteristic of having thick air gap is considered in the field-circuit 2D model. The co-simulation using state equation and time-step finite element equation is used, the time step of the state equation is smaller than that of the time-step finite element equation. PWM-VI-PMLSM and S-VS-PMLSM have the same current periodicity and similar current amplitude. The current of SPWM-VI-PMLSM has various harmonic components distorted as a result of magnetic saturation and non-sinusoidal air gap field. The tangential electromagnetic thrust of SPWM-VI-PMLSM under steady state oscillate with a period decided by pole pitch, and it has various harmonic components dampening thrust fluctuation, Thus S-VS-PMLSM has better performance than SPWM-VI-PMLSM. S-VS-PMLSM and SPWM-VI-PMLSM have the same periodicity of slip fluctuation, the slip value of SPWM-VI-PMLSM is larger than that of S-VS-PMLSM. The simulation results accords with experimental data.

Index Terms—Permanent magnet linear synchronous motor (PMLSM), sinusoidal pulse width module voltage source, field-circuit coupled method, time-stepping finite element method, magnetic flux density, performances analysis

I. INTRODUCTION

With the rapid development of permanent magnet material, power electronic technology, microelectronic technology, the performance of permanent magnet linear motor (PMLSM) tends to be more excellent. PMLSM has advantages of positioning precision, high force density achievable, loss thermal losses, and high thrust-force capability. Furthermore, there is increasing demand for positioning precision in horizontal translation system and many attentions have been focused on PMLSM. Yet inverters composed of switch arrays provide non-sinusoidal voltage or current, and the structural performances of the tooth-slot and winding distribution of the motor could lead to a mass of harmonic components, these factors can cause the parametric change of the motor, thrust fluctuation, loud noise, sharp winding temperature rise, severely deteriorating the motor performance^[1-6].

There are a lot of literatures about the study of performances of PMLSM fed by sinusoidal current source, namely the current density distribution of the current source is known, and the finite element method is adopted to solve the equations. In Ref. [7-11], the performances of PMLSM fed by sinusoidal current source are studied. To overcome deficiency in performances analysis of PMLSM using numerical method and analytical method, hybrid method combined with finite element method (FEM) and analytical solution were adopted because fast and accurate analysis of the field is necessary for PMLSM. Electromotive force without load and magnetic link with the mover position are attained, and the performances of PMLSM applied SPWM-VI was profoundly researched [12]. Specifications such as current, speed and thrust force should be largely changed, when permanent magnet linear synchronous motor happen to load sudden changing. Using state variable method based on inductance matrix to analyze the characteristics of motor happens to load sudden changing. The results show that main factor of speed fluctuation in steady operation condition is end component of detent force, windings resistance effects power angle curve and the motor can

Manuscript received November 1, 2011; revised November 30, 2011; accepted December 10, 2011.

The authors are greatly indebted to Doctoral Program of Higher Education Research Fund for new teachers funding China Ministry of Education (20104116120001), National Natural Science Foundation of China (NO. 61074095), Natural Science Program of Henan province Education Department in 2011(2011A470003), 2011 year guidance of scientific and technological research projects of China Coal Industry Association (MTKJ2011-391) for its support and Henan polytechnic university doctor fund project (B2010-53) for its support.

Corresponding author: Jikai SI. E-mail: sijikai527@126.com

work at first or third quadrant region [13]. In Ref. [14], the time-stepping finite element method is adopted to study the performances of PMLSM fed by PWM power source with secondary conductive plane; it only presents the simulation results of the thrust and the current. In Ref. [15-16], the time-stepping finite element method is adopted to study the performances of PMLSM supplied by SVPWM voltage source inverter, and the simulation figures of voltage and current, the simulation result and experimental result of velocity and displacement are presented. The high-frequency component mathematical models of an interior permanent magnet synchronous motor (IPMSM) were analyzed in two stationary reference frames. A rotor position sensorless control strategy was studied using carrier frequency component method. In order to provide continuous carrier frequency component signals, three-phase triangular carrier SPWM was adopted. The carrier frequency component current (CFCC) equations of the IPMSM were deduced under the modulating pattern. The peak expressions of CFCC contained the rotor position information. Based on the information, the position sensorless control of IPMSM was built. The simulation and experimental results demonstrate that the proposed method can realize position sensorless control of IPMSM over full speed range [17]. Yet the performances of PMLSM supplied by SPWM inverter need to be studied further.

When studying the characteristic of motor supplied by voltage source inverter, the current iteration method is often adopted to solve the problem of voltage constraint, which has slow convergence and poor effect, so in this paper, the field-circuit coupled time-stepping finite element method is adopted to have a further study of the performances of PMLSM supplied by SPWM voltage source inverter. The co-simulation has greatly reduced the time for simulation and improved the precision of simulation, and the simulation results are presented at last and validated with the experimental data.

A. Physical Model of PMLSM

The primary of PMLSM is composed of three-phase windings and the primary iron yoke with rectangular slots, and the secondary is composed of permanent magnets (Neodymium Iron Boron) and magnetic isolation blocks that are placed on the steel plate. The PMLSM studied in this paper is a single side and planar type non-salient pole motor with long secondary and short primary, as is shown in Figure 1. In the non-salient pole structure, the magnetization direction of the permanent magnets is concordant with the direction of the air gap flux axis, and has lower pole-to-pole flux leakage and simple craftwork. The specifications of PMLSM are shown in Tab. 1.

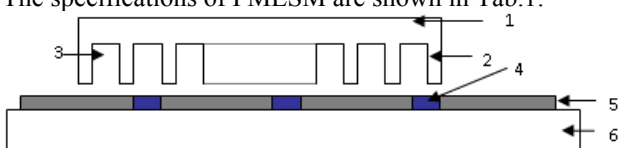


Figure 1. Physical model (Non-salient pole structure)

1. Primary yoke 2.Tooth 3.Slot 4.Magnetic isolation block 5.Permanent magnet 6.Secondary yoken.

TABLE I.
PMLSM SPECIFICATIONS

	Items	Value
Primary	Phases	3
	Turns	90
	Armature material	iron
	Pole pitch	39mm
	Slot pitch	13mm
	Wire running method	Integral pitch/Double layer
	Tooth pitch	13mm
Secondary	PM material	NdFeB
	PM width	27mm
	PM height	7mm
	PM length	120mm
	PM placement	Surface fix
Air gap	Mechanical	8mm
Rated thrust		65Kg

II. FIELD-CIRCUIT COUPLED MATHEMATICAL MODEL OF PMLSM

To take the external circuit fed by SPWM voltage source inverter and the motor end effect into account, this paper adopts field-circuit coupled method to calculate the electromagnetic transient process, solve equation variables of magnetic vector potential and the motor phase current, which are the combination of electromagnetic field time-step finite element equations and three-phase winding circuit equations by electromotive force in the armature windings.

The transient field equation in which A denotes magnetic vector potential is shown as (1) according to Maxwell equations.

$$\frac{\partial^2 A}{\partial x^2} + \frac{\partial^2 A}{\partial y^2} = -\mu J_s - \mu J_m \quad (1)$$

Where A is z-axis component of magnetic vector potential, J_s is Current density of the primary windings, J_m is Equivalent magnetizing surface current density of permanent magnet, μ is the permeability.

In this paper, the model is subdivided into small triangle elements to form a mesh and adopts n-order unit basic function and linear interpolation. After applying the Galerkin method, the governing equations for the analysis model is expressed as follows.

$$[[S]] - [C] \begin{bmatrix} [A] \\ [I] \end{bmatrix} + \frac{\partial}{\partial t} [[T] [0]] \begin{bmatrix} [A] \\ [I] \end{bmatrix} = [G] \quad (2)$$

Where A is unknown node magnetic vector potential, I is current in the windings, S , C , T is coefficient matrix, G is matrix of equivalent magnetization current density.

Equivalent magnetizing surface current method is adopted to deal with NdFeB type permanent magnet with uniformity magnetization, regulation shape, linear demagnetization and intensity of magnetization of M_0 .

$$J_m = \frac{M_0}{\mu_0} \quad (3)$$

The resistance and leakage reactance of PMLSM is not neglected due to the characteristic of having thick air gap. According to the Ohm law and the Faraday electromagnetic induction law, relation of electromotive force and voltage produced the primary three-phase windings is shown in (4).

$$\frac{d}{dt}[\psi] + [L_l] \frac{d}{dt}[I] + [R][I] = [U]. \quad (4)$$

Where ψ is the windings flux linkage, L_l is the motor leakage inductance, R is windings resistance, and U is windings phase voltage.

$$\psi = N \int_{S_2} B \cdot dS = N \oint_l A \cdot dl. \quad (5)$$

$$J_s = \frac{I}{S_1}. \quad (6)$$

Where N is winding effective turns, B is flux density, S_1 is winding effective area in the slot, S_2 is coupled effective area of the primary and the secondary.

Maxwell's stress tensor is adopted to calculate PMLSM electromagnetic force, which includes all kinds of harmonics component electromagnetic force. The tangential component of the force is shown in (7).

$$F_{thrust} = \frac{L_1}{\mu_0} \int_0^{L_2} (-B_x B_y) dx. \quad (7)$$

The motor electromagnetic force normal component is shown in (8).

$$F_{normal} = \frac{L_1}{\mu_0} \int_0^{L_2} \frac{1}{2} (B_x^2 - B_y^2) dx. \quad (8)$$

Where L_1 is winding effective length, L_2 is integrating range, B_x is x-axis flux density component in the air gap field, B_y is y-axis flux density component in the air gap field, F_{normal} is electromagnetic thrust force, F_{thrust} is normal electromagnetic force.

Movement equation of PMLSM is shown in (9).

$$F_{thrust} = m \frac{dv}{dt} + F_L. \quad (9)$$

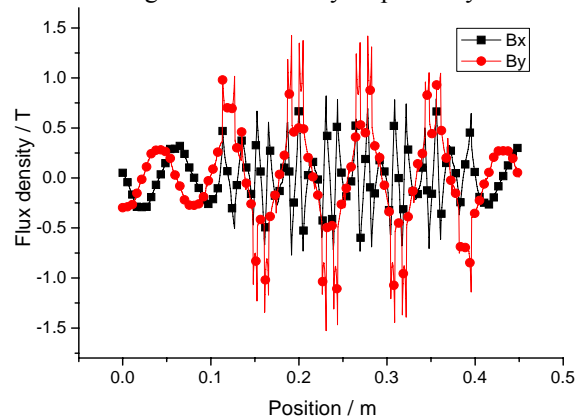
Where m is mass, v is the motor mover velocity, F_L is load force.

III. ANALYSIS OF STEADY-STATE PERFORMANCES OF PMLSM

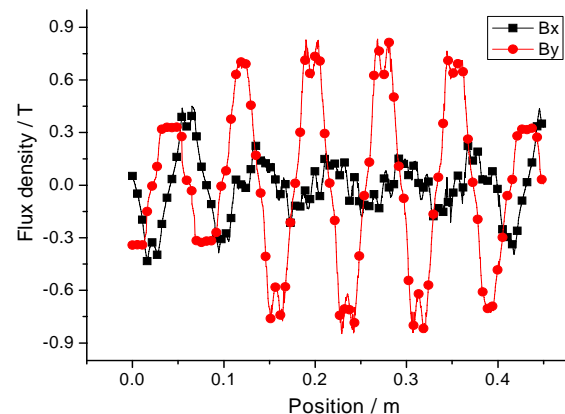
In order to know the cause of electromagnetic thrust and mover velocity fluctuation of low-velocity PMLSM fed by SPWM-VS, the steady-state performances of low-velocity PMLSM are analyzed.

The magnetic field distribution is the result of the joint action of the primary windings and secondary permanent

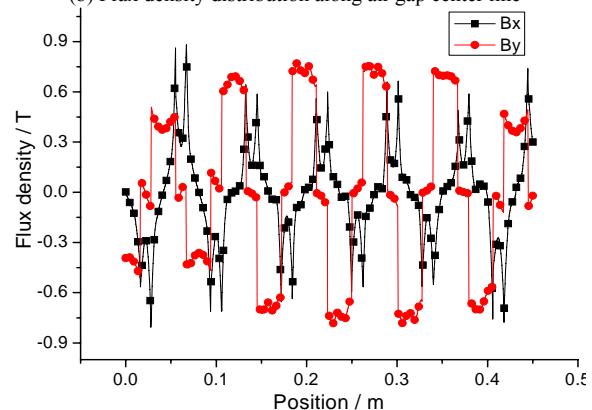
magnet of PMLSM, the field distribution and variation in different media and its linkage with current decide the electromagnetic parameters and the performance of PMLSM. Figure 2 and Figure 3 show the result of calculation of magnetic flux density on the primary surface, air gap centerline and the permanent magnet surface of SPWM-VI-PMLSM and S-VS-PMLSM respectively. B_x and B_y in the figures denote tangential and normal magnetic flux density respectively.



(a) Flux density distribution on primary tooth-slot surface

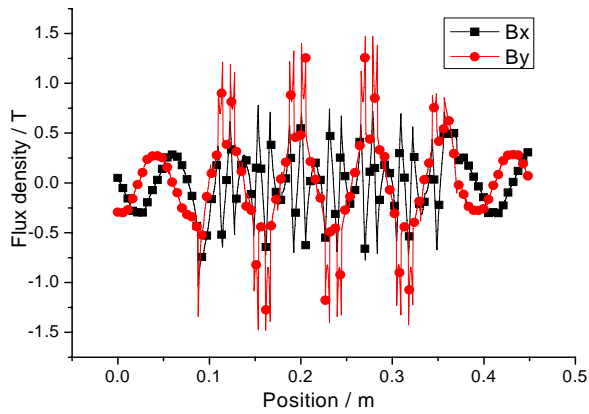


(b) Flux density distribution along air gap center line

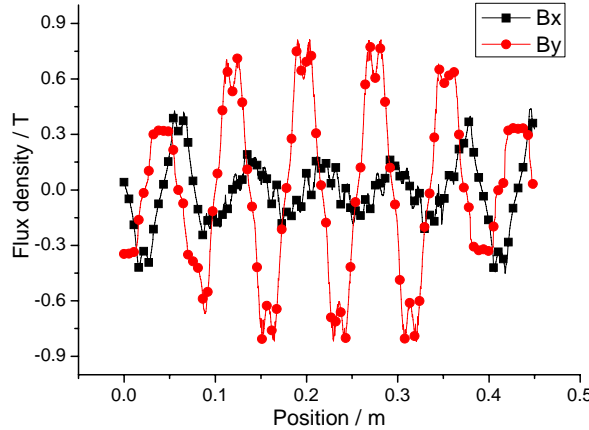


(c) Flux density distribution on the permanent magnet surface

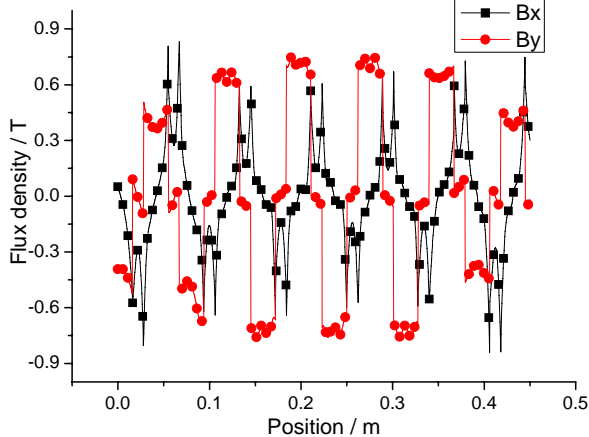
Figure 2. Calculation result of the flux density distribution of SPWM-VI-PMLSM



(a) Flux density distribution on the primary tooth-slot surface



(b) Flux density distribution along air gap center line



(c) Flux density distribution on the permanent magnet surface

Figure 3. Calculation result of the flux density distribution of S-VS-PMLSM

Figure 4 shows the velocity curve from starting to steady state of SPWM-VI-PMLSM and PMLSM fed by sinusoidal voltage source in load 100.0N condition.

In Figure 4, S-VS denotes the sinusoidal voltage source, SPWM-VI denotes the sinusoidal pulse width modulation voltage inverter. It can be seen from the figure that the mover velocity of SPWM-VI-PMLSM and S-VS-PMLSM oscillate around the synchronous velocity of 0.156m/s, the oscillation period under the steady state condition is 0.25s, and the oscillation amplitude of SPWM-VI-PMLSM is 10.93% larger than that of S-VS-

PMLSM. The oscillation range of the mover velocity of SPWM-VI-PMLSM is 0.09719m/s~0.21481m/s, the oscillation range of the mover velocity of S-VS-PMLSM is 0.10912m/s~0.20288m/s. Thus it can be seen that the supply harmonic is not the major cause of mover velocity oscillation of PMLSM. The calculation results of magnetic co-energy of SPWM-VI-PMLSM and S-VS-PMLSM are shown in Figure 5 Figure 6 shows the calculation results of the load angle (the distance between the centerline of the primary armature field and the mover field) of S-VS and SPWM-VI-PMLSM.

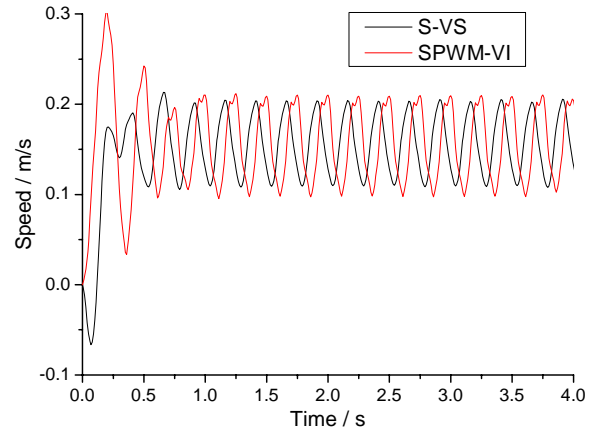


Figure 4. Mover velocity calculation result of PMLSM driven by S-VS and SPWM-VI

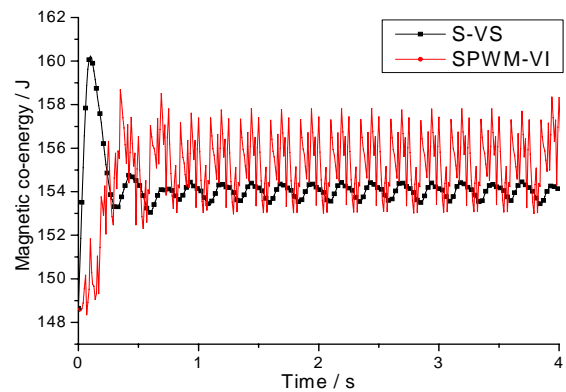
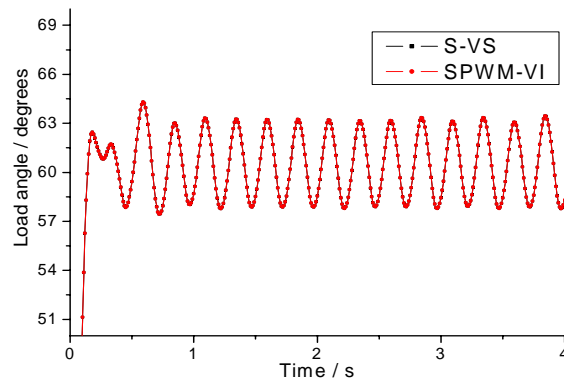


Figure 5. Calculation result of magnetic co-energy



e 6. Calculation result of load angle

Figur

It can be seen from Figure 5 that the magnetic co-energy of SPWM-VI-PMLSM has various harmonic components; the magnetic co-energy of S-VS-PMLSM

under steady state condition has better sine degree, the harmonic components of SPWM-VI-PMLSM made its own contribution to the magnetic co-energy. It can be seen from Figure 6 that the load angle of SPWM-VI-PMLSM system and S-VS-PMLSM dose not vary at the same load condition, the load angle has nothing to do with the form of voltage. Figure 7 and Figure 8 show the calculation results of A-phase current and A-phase terminal voltage of SPWM-VI and S-VS.

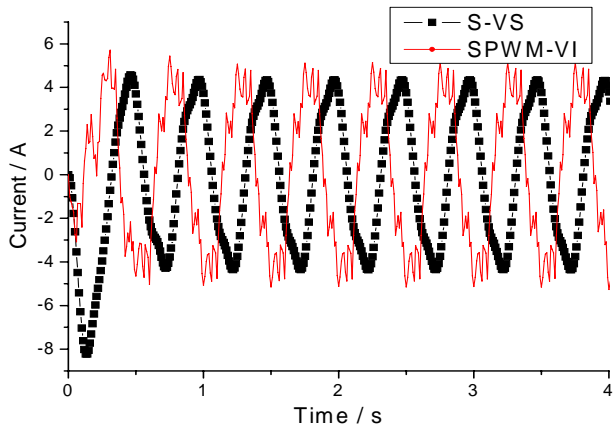


Figure 7. A-phase current

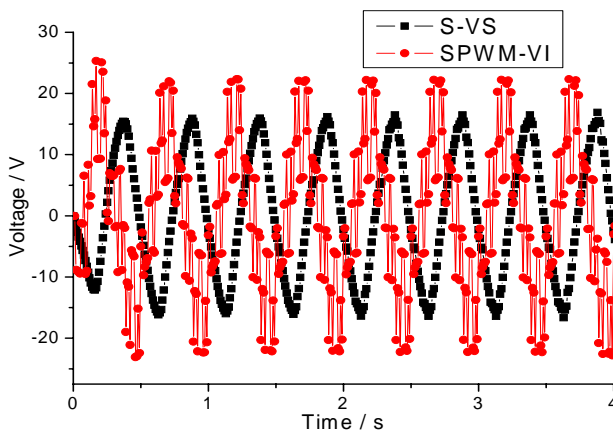


Figure 8. A-phase terminal voltage

It can be seen from Figure 7 that PWM-VI-PMLSM and S-VS-PMLSM have the same current periodicity and similar current amplitude at A-phase. The current of SPWM-VI-PMLSM has various harmonic components, the current of S-VS-PMLSM is distorted as a result of magnetic saturation and non-sinusoidal air gap field, and it is not simple sinusoidal current. It can be seen from Figure 8 that the phase voltage of S-VS-PMLSM has better sine degree, while the phase voltage of SPWM-VI-PMLSM has various harmonic components, and is 26.1% larger than that of S-VS-PMLSM. Figure 9 shows the calculation result of electromagnetic thrust of SPWM-VI-PMLSM and S-VS-PMLSM.

It can be seen from Figure 9 that the tangential electromagnetic thrust of S-VS-PMLSM under steady state has better sine degree, oscillate around the value of 100.00N with a period decided by pole pitch, the oscillation amplitude is 267.00N. The tangential electromagnetic thrust of SPWM-VI-PMLSM under

steady state oscillate around the value of 112.29N with a period decided by pole pitch, the oscillation amplitude is 393.21N, and it has various harmonic components. Thus it can be seen that for dampening thrust fluctuation, S-VS-PMLSM has better performance than SPWM-VI-PMLSM.

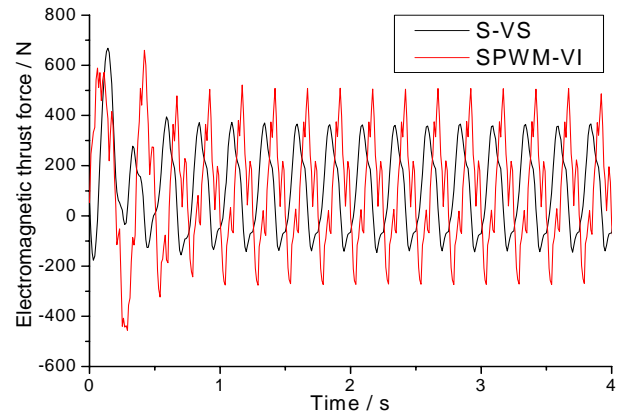


Figure 9. Calculation result of the electromagnetic thrust

Figure10 shows the calculation result of A-phase winding flux linkage of SPWM-VI-PMLSM and S-VS-PMLSM. Figure11 shows the calculation result of slip curve of SPWM-VI-PMLSM and S-VS-PMLSM.

It can be seen from Figure10 that the difference of the value of A-phase winding flux linkage between S-VS-PMLSM and SPWM-VI-PMLSM is very slight, for the waveform, the A-phase winding flux linkage of S-VS-PMLSM has better sine degree.

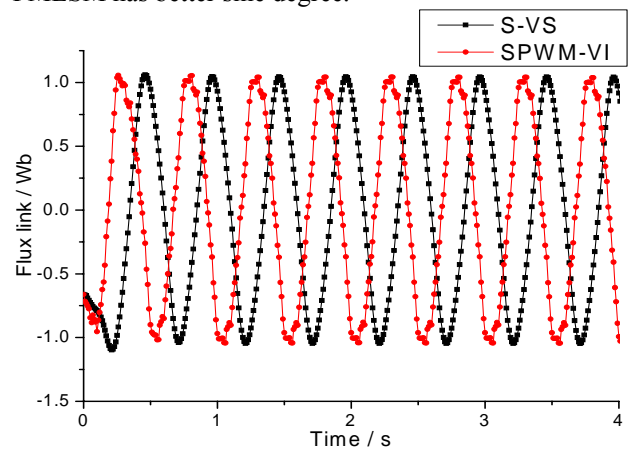


Figure 10. Calculation result of A-phase winding flux linkage

It can be seen from Figure11 that S-VS-PMLSM and SPWM-VI-PMLSM have the same periodicity of slip fluctuation, yet the slip value of SPWM-VI-PMLSM is 24.6% larger than that of S-VS-PMLSM. Figure12, Figure13, Figure14 show the experimental curve of SPPMLSM fed by SPWM-VI with the carrier frequency of 0.7 kHz, they show the experimental curve of phase voltage, velocity and electromagnetic thrust respectively.

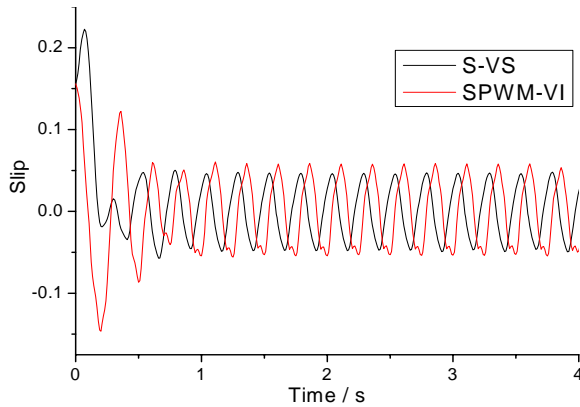


Figure 11. Calculation result of slip

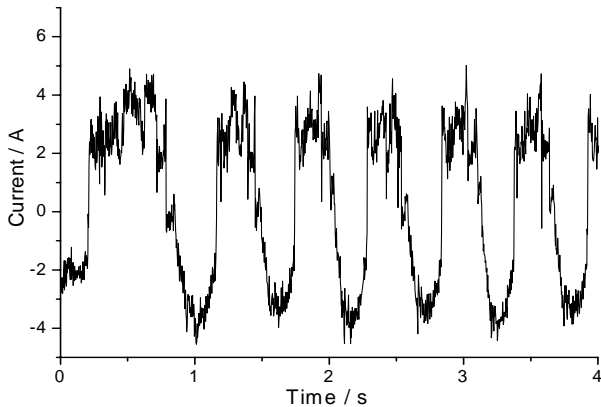


Figure 12. Experimental current of the phase-A winding of the primary

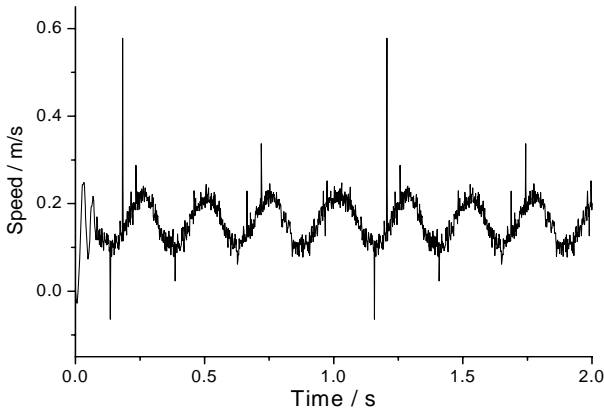


Figure 13. Experimental curve of mover velocity

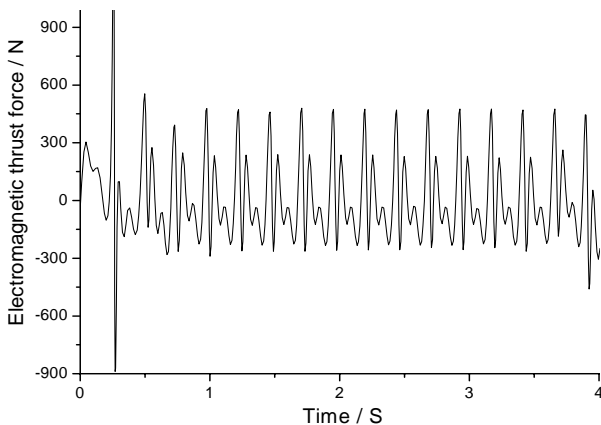


Figure 14. Experimental curve of mover thrust

The burr on the experiment curve of velocity is caused by measurement noise.

IV. CONCLUSIONS

For the open-loop scalar and constant flux controlled running mode of PMLSM, to study the performances of PMLSM using field-circuit coupled time-stepping method is feasible, and the co-simulation using state equation and field finite element equation is adopted, it has reduced the time for simulation and improved the precision of simulation. The following conclusions are drawn.

1. The mover velocity of SPWM-VI-PMLSM and S-VS-PMLSM oscillate around the synchronous velocity of 0.156m/s, the oscillation period under the steady state condition is 0.25s, and the oscillation amplitude of SPWM-VI-PMLSM is 10.93% larger than that of S-VS-PMLSM. The oscillation range of the mover velocity of SPWM-VI-PMLSM is 0.09719m/s~0.21481m/s, the oscillation range of the mover velocity of S-VS-PMLSM is 0.10912m/s~0.20288m/s. Thus it can be seen that the supply harmonic is not the major cause of mover velocity oscillation of PMLSM.

2. PWM-VI-PMLSM and S-VS-PMLSM have the same current periodicity and similar current amplitude at A-phase. The current of SPWM-VI-PMLSM has various harmonic components, the current of S-VS-PMLSM is distorted as a result of magnetic saturation and non-sinusoidal air gap field, and it is not simple sinusoidal current.

3. The phase voltage of S-VS-PMLSM has better sine degree, while the phase voltage of SPWM-VI-PMLSM has various harmonic components, and is 26.1% larger than that of S-VS-PMLSM.

4. S-VS-PMLSM and SPWM-VI-PMLSM have the same periodicity of slip fluctuation, yet the slip value of SPWM-VI-PMLSM is 24.6% larger than that of S-VS-PMLSM.

The simulation results are verified by comparing and analyzing the simulation data and experimental data.

ACKNOWLEDGMENT

The authors are greatly indebted to Doctoral Program of Higher Education Research Fund for new teachers funding China Ministry of Education (20104116120001), National Natural Science Foundation of China (NO. 61074095), Natural Science Program of Henan province Education Department in 2011(2011A470003), 2011 year guidance of scientific and technological research projects of China Coal Industry Association (MTKJ2011-391) for its support and henan polytechnic university doctor fund project (B2010-53) for its support.

REFERENCES

- [1] Wang Jiabin, Wang Weiya, Atallah, Kais, "A linear permanent-magnet motor for active vehicle suspension", IEEE Transactions on Vehicular Technology, v 60, n 1, p 55-63, January 2011.

- [2] Tavana, Nariman Roshandel ; Shoulaie, Abbas, "Pole-shape optimization of permanent-magnet linear synchronous motor for reduction of thrust ripple", *Energy Conversion and Management*, v 52, n 1, pp. 349-354, January 2011.
- [3] Zhao Jinghong, Zhang Junhong, Fang Fang, Gao Wei, "Analytical calculation of magnetic field and thrust force in radial magnetized tubular permanent magnet linear synchronous motor", *Diangong Jishu Xuebao/Transactions of China Electrotechnical Society*, v 26, n 7, pp. 154-160, July 2011.
- [4] Si Ji-Kai, Wang Xu-Dong, Yuan Shi-Ying, Ma Xing-He, Chen Hao, "Non-linear model establishment and steady state characteristics analysis of permanent magnet linear synchronous motor", *Journal of the China Coal Society*, v 35, n 2, pp. 343-348, February 2010.
- [5] Si Ji-Kai, Chen Hao, Wang Xu-Dong, Yuan Shi-Ying, Jiao Liu-Cheng, "Analysis and reduction technique of the end component of detent force in flat permanent magnet linear synchronous machine", *Proceedings of the Chinese Society of Electrical Engineering*, v27, n SUPPL., pp. 132-136, December 2007.
- [6] Kim Yong-Jae, Watada Masaya, Dohmeki Hideo, "Reduction of the cogging force at the outlet edge of a stationary discontinuous primary linear synchronous motor", *IEEE Transactions on Magnetics*, v 43, n 1, January, 2007, pp. 40-45
- [7] Wang Xudong, Yuan Shiyong, Jiao Liucheng, "3-D analysis of electromagnetic field and performance in a permanent magnet linear synchronous motor", *IEMDC 2001. IEEE International*, pp. 445-447, 2001.
- [8] Sanada M., Morimoto S., Takeda Y., "Interior permanent magnet linear synchronous motor for high-performance drives", *IEEE Transactions on Industry Applications*, Volume 33, Issue 4, pp. 966-972, 1997.
- [9] Sang-Yong Jung, Jang-Sung Chun, Hyun-Kyo Jung, "Performance evaluation of slotless permanent magnet linear synchronous motor energized by partially excited primary current", *IEEE Transactions on Magnetics*, Volume 37, Issue 5, Part 1, Sept. 2001, pp. 3757-3761, 2001.
- [10] Sang-Yeop Kwak, Jae-Kwang Kim, Hyun-Kyo Jung, "Characteristic Analysis of Multilayer-Buried Magnet Synchronous Motor Using Fixed Permeability Method", *IEEE Transaction on Energy Conversion*, Vol.20, No.3, September 2005, pp. 549-555, 2005.
- [11] Gyu-Hong Kang, Jin Hur, Byoung-Kuk, "Force Characteristic Analysis of PMLSMs for Magnetic Levitation Stage Based on 3-Dimensional Equivalent Magnetic Circuit Network", *IAS 2004*, pp. 2099-2104, 2004.
- [12] Si Ji-Kai, Feng Hai-Chao, Xu Xiao-Zhuo, Wang Xu-Dong, Yuan Shi-Ying, "Performances analysis of permanent magnet linear synchronous machine using hybrid method combing FEM and analytical solution", *Dianji yu Kongzhi Xuebao/Electric Machines and Control*, v 14, n 10, pp. 8-14+20, October 2010
- [13] Si Ji-Kai, Wang Xu-Dong, Jiao Liu-Cheng, Yuan Shi-Ying, Chen, Hao, "Load sudden change and steady state oscillation characteristics of permanent magnet linear synchronous motor", *Electric Machines and Control*, v 13, n 4, pp. 483-489, July 2009
- [14] Jung In-Soung, Hyun Dong-Seok, "Dynamic performances of PM linear synchronous motor driven by PWM inverter by finite element analysis," *IEEE Transactions on Magnetics*, v 35, n 5 pt 2, Sep, 1999, pp. 3697-3699, 1999.
- [15] Kwon Byung Il, Woo Kyung Il, Kim Duck Jin, Park, Seung Chan, "Finite element analysis for dynamic performances of an inverter-fed PMLSM by a new moving mesh technique", *IEEE Transactions on Magnetics*, v 36, n 4 I, Jul, 2000, pp. 1574-1577, 2000.
- [16] Si Jikai, Chen Hao, Wang Xudong, Yuan Shiyong, Shanguan Xuanfeng. "Load performance of PMLSM in lower speed region fed by sinusoidal PWM inverter", *Diangong Jishu Xuebao/Transactions of China Electrotechnical Society*, v23, n9, pp. 58-64, September 2008
- [17] Gao Hong-Wei, Yu Yan-Jun, Chai Feng, Cheng Shu-Kang. "Position sensorless control of interior permanent magnet synchronous motor based on carrier frequency component method", *Proceedings of the Chinese Society of Electrical Engineering*, v30, n18, pp.91-96, 2010



Jikai Si was born in Henan Province, China, in 1973. He received the B.Eng. and M. Eng. degrees from Jiaozuo Institute and Technology, Henan Polytechnic University, Jiaozuo, China, in 1998 and 2005, respectively. He received the Ph.D. degree in The School of Information and Electrical Engineering at China University of Mining and Technology, Xuzhou, China.

Currently, he is a lecture in the Henan Polytechnic University. His main research interests include the theory, application and control of special motor.

From 2007 to 2008, he was with ASM Pacific Technology Ltd., HongKong, as a Research Engineer. Now, he is a teacher in School of Electrical Engineering and Automation, Henan Polytechnic University, china.

Dr. SI is a member of institute of linear electric machine and drives, Henan Province, China. In recent years, he participates in 8 provincial and 4 country research projects, published more than 16 academic papers.



Xiaozhuo Xu was born in China in 1980, and received the B.S. and M.S. degrees in electrical engineering and automation, motor and electrical from School of Electrical Engineering and Automation, Henan Polytechnic University, china, in 2003 and 2006, respectively. His research interests are the analysis of physical field for special motor, optimization design of linear and

rotary machines.

Now, he is a teacher in School of Electrical Engineering and Automation, Henan Polytechnic University, china.

Mr. Xu is a member of institute of linear electric machine and drives, Henan Province, China. In recent years, he participates in 8 provincial and 2 country research projects, published more than 10 academic papers.



Haichao Feng was born in China in 1983, and received the B.S. and M.S. degrees in electrical engineering and automation, control theory and control engineering from School of Electrical Engineering and Automation, Henan Polytechnic University, china, in 2005 and 2008, respectively. His research interests are the optimization design of

linear and rotary machines, power electronics, and their controls.

New, he is a teacher in School of Electrical Engineering and Automation, Henan Polytechnic University, china.

Mr. FENG is a member of institute of linear electric machine and drives, Henan Province, China. In recent years, he participates in 5 provincial and 2 country research projects, published more than 8 academic papers.



Baoyu Xu was born in Jiaozuo city, Henan Province, China in 1963, and received the PH.D degree in mechanical design and manufacturing from College of Mechanical & Electrical Engineering, Central South University, China, in 2011. His research interests are stochastic vibration and dynamic behavior of mechanical systems.

Since 1996, He has been working in School of Mechanical and Power Engineering, Henan Polytechnic University, china mainly engaged in teaching and scientific research.

Dr. Xu is a member of institute of linear electric machine and drives, Henan Province, China.



Xudong Wang was born in China in 1967, and received the PH.D degree in electrical engineering from School of Electrical engineering, Xi'an Jiaotong University, China, in 2002. His research interests are linear motor theory and control, motor optimization, energy efficient motors.

He is a Professor of electrical engineering and Vice-dean in School of Electrical Engineering and Automation, Henan Polytechnic University, china. As the Director of Institute of Linear Motor and Drive in Henan Polytechnic University, he achieved 30 research projects, including 4 the National Natural Science Foundation of China, and over 80 papers was published, among which over 20 was embodied by EI and SA. He has 13 national invention patents and 9 utility model authorization patents in China. He presided to develop many experimental system or products, such as rope-less hoist system with high-power, home elevator driven by PMLSM, automatic precision servo system, high temperatures superconducting Maglev vehicles, efficient asynchronous motor, self-starting PM motor, and so on. Now, he has 9 projects are being undertaken about multi-car rope-less hoist system driven by PMLSM.